

FUZZY CONTROL OF INTEGRATED CURRENT CONTROLLED CONVERTER-INVERTER FED CAGE INDUCTION MOTOR DRIVE

B.N. Singh, Student member IEEE. Bhim Singh and B.P. Singh. SM IEEE
Department of Electrical Engineering, HT Delhi, Hauz Khas
New Delhi 110 016, INDIA

Abstract-The paper presents the performance analysis of a vector controlled cage induction motor drive. The drive is fed from a current controlled converter- inverter system. The switching technique being used in control of the converter as well as inverter is PWM current control. Closed loop control of the cage induction motor utilizes fuzzy PID speed controller. The advantages offered by the current control converter- inverter link are exploited. In order to examine the dynamic performance of the drive system its model is simulated and results are analyzed. The potential applications of this particular drive system are outlined.

Key Words: Induction motor, Fuzzy controller, Vector control, Adjustable power factor.

I. INTRODUCTION

Vector controlled induction motor drive offers better dynamic performance [1] and it is widely used in a number of industrial applications. Normally, a vector controlled cage motor is fed from a current/voltage controlled inverter [2-3]. This drive requires fast regulation of the currents through its windings [4-7]. For this the current controlled voltage source inverter [2] is normally being employed owing to its capability of regulating the motor currents in a desired manner. The diode bridge rectifier feeding power to the current controlled inverter has its own demerits and limitations [8-10] such as 'lower power factor', 'distortion in input current waves', 'harmonics injection in the AC mains which pollutes the supply system' and 'no possibility of regeneration of energy? In order to overcome these problems the diode bridge rectifier is currently being replaced by a current controlled converter [1, 8-10].

The current controlled converter has some advantages [8-10] such as it can operate at adjustable power factor and can provide inherent regeneration of the energy owing to the bi-directional power flow. Moreover, currents input to the converter have sinusoidal shape and therefore, there is negligible pollution of the supply system from unwanted harmonics. In essence, the current controlled converter-inverter link functions as an ideal frequency changer.

The control of the integrated converter-inverter system feeding power to the cage motor has become easier due to advancement in the semiconductor technology [11-12] resulting in high frequency switches along with signal sensing and signal processing techniques. With the existing devices (MOSFET, IGBT and MCT) and processors (Micro processors, microcomputers and DSPs), the structure of proposed drive system appears to be simpler, however, its analysis is more challenging as in this case the number of system's parts and variables get increased.

In this paper the current controlled converter- inverter fed vector controlled [13] cage induction motor drive system has been modeled and simulated. While selecting the operating voltage of the current controlled converter, the loss of control limit and distortion limit [9] are respected. The design of a fuzzy PID speed controller [14-15] is explained systematically. The potential applications of such a drive system are identified.

II. CONTROL STRATEGY

Fig.1 shows the schematic of the proposed drive system. The

current controlled converter operates at adjustable power factor while feeding power to the current controlled inverter. The inverter operates at variable voltage and variable frequency and supplies power to the induction motor.

In closed loop control of converter, the DC link voltage (v_j) is sensed and is compared with the set reference (V_j) voltage. The PID voltage regulator processes the resulted error (y_j). I_1 is the output of the PID voltage regulator. This loop is called as the DC link voltage feedback loop. Apart from this a load feedforward loop is also incorporated in order to have faster regulation of converter currents along with the rapid control of DC link voltage. The output power estimator used in load feedforward loop provides an output (I_j which is added with I_1). Further I_1 and I_2 together form the magnitude (I_j) of the three phase reference currents (i_a^* , i_b^* and i_c^*). Three phase voltages (e_a , e_b and e_c) at the converter input are sensed and therefrom, the unit current templates (u_a , u_b and u_c) are generated. In order to decide the phase of currents input to converter (i_a , i_b and i_c) with respect to the corresponding voltages (e_a , e_b and e_c), the unit current templates (u_a , u_b and u_c) are given a desired phase shift ' θ^* '. The current templates are multiplied with the I_j , and resulted quantities are three phase reference currents (i_a^* , i_b^* and i_c^*) at converter input.

In this investigation the converter is operated at unity power factor i.e. phase shift ' θ ' is set at zero. The currents (i_a^* , i_b^* and i_c^*) are the ideal currents to be maintained at the input of the converter. Accomplishing the same the currents in two phases at converter input are sensed and thereafter, current in the third phase is derived. This gives the three phase currents (i_a , i_b and i_c) at the input port of the converter. These currents (i_a , i_b and i_c) are compared with the reference currents (i_a^* , i_b^* and i_c^*) in the PWM current controller. As a result of this comparison a fast switching (ON/OFF) pattern is generated which controls the ON/OFF times of the converter valves (solid state semiconductor switches) and the currents input to converter exactly track the reference currents. It is noted here that in order to facilitate bi-directional power flow through a semiconductor switch (IGBT in the present investigation) a high frequency diode is connected in anti-parallel with the switch.

For the closed loop control of the induction motor its sensed speed (ω_r) is compared with the set reference speed (ω_r^*). Speed error (w_e) so obtained is processed in the fuzzy PID speed controller in the regular sampling interval. The output of the speed controller is the reference torque (T^*). The reference magnetizing current vector (i_{mr}^*) is worked out in the field weakening block.

The quantities T^* and i_{mr}^* are further processed to work out the quadrature reference currents (i_j^* and i_v^*) and reference slip speed (w_2^*). The currents (i_j^* and i_v^*) and slip speed (w_2^*) are input to the field orientation block.

The currents ($i_{M'}^*$ and i_v^*) are given in synchronously rotating reference frame. Park's transformation changes the currents (i_j^* and i_v^*) into quadrature currents (i_j^* and i_v^*) in stationary reference frame. Applying two phase to three phase transformation one gets three phase reference currents (i_a^* , i_b^* and i_c^*). The field oriented control structure completes this job.

The currents (i_a^* , i_b^* and i_c^*) are the ideal currents to be maintained in the motor windings in order to accomplish its vector

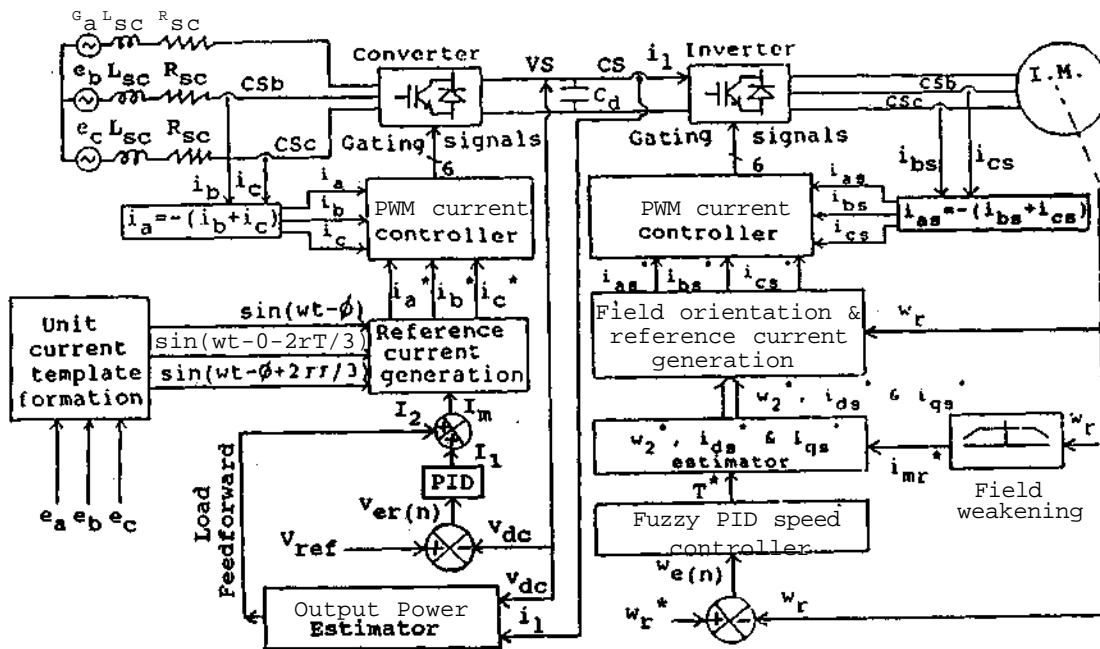


Fig.1 schematic of integrated current controlled converter-inverter fed vector controlled cage induction motor drive

control. The two phase currents out of the input currents to the motor are sensed and the current in the third phase is derived, this results in three phase currents (i_a , i_b and i_c) input to the motor. These currents (i_a , i_b and i_c) are compared with the reference currents (i_a^* , i_b^* and i_c^*) in the PWM current controller. This comparison leads to the generation of a switching (ON/OFF) pattern. This switching pattern controls the currents flowing through inverter devices such that the three phase currents (i_a , i_b and i_c) output to the motor track exactly the three phase reference currents (i_a^* , i_b^* and i_c^*). In response to these currents (i_a , i_b and i_c) the motor runs stably at set speed. During transients the reference currents (i_a^* , i_b^* and i_c^*) change quickly and due to fast acting PWM current controller motor currents (i_a , i_b and i_c) remain in close vicinity of them. This, therefore, results in a fast dynamic response of the drive.

III. SYSTEM MODELING

The proposed drive system is shown in Fig.1. It consists of the power source i.e. current controlled converter and its various parts, current controlled inverter and its parts, speed controller, field oriented control structure and PWM current controller. Each one of these parts is modeled separately and are then joined together to have the complete model of the proposed drive system.

A. Converter System

The schematic of current controlled converter is shown in Fig.2. Three phase AC source provides the input to the converter and DC is at its output. The induction motor load is connected at the output of the

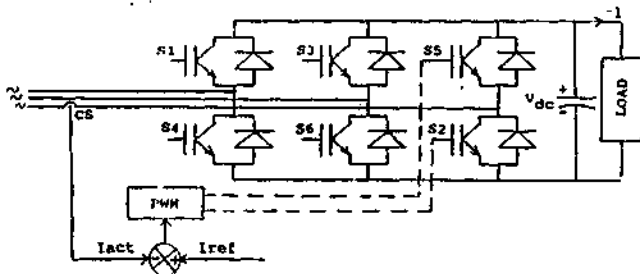


Fig.2 schematic of PWM current controlled converter

converter through current controlled inverter.

Converter operating in the current controlled mode is represented by the following mathematical equations;

$$p i_a = -(R_c/L_c) i_a + (e_a - v_a)/L_c \quad (1)$$

$$p i_b = -(R_c/L_c) i_b + (e_b - v_b)/L_c \quad (2)$$

$$p i_c = -(R_c/L_c) i_c + (e_c - v_c)/L_c \quad (3)$$

$$p v_{dc} = I_c/QCA'SAC + i/SBC + i_c'SCC - U \quad (4)$$

Where R_c and L_c are per phase resistance and inductance, respectively, of the AC source. SAC, SBC and SCC are the switching functions stating the ON/OFF positions of three phase converter's switches, and i_c is the load current at converter output.

The DC link voltage (v_{dc}) is reflected in the form of the three phase stepped AC voltages (v_a , v_b and v_c) as a result of fast ON/OFF of the converter switches, thereby, controlling the currents through these switches in a desired manner.

The reflected three phase instantaneous AC voltages (v_a , v_b and v_c) at the input of the converter are expressed in terms of instantaneous DC link voltage (v_{dc}) and converter switching functions. These relations are given below:

$$v_a = v_{dc}/3 * (2 * SAC - SBC - SCC) \quad (5)$$

$$v_b = v_{dc}/3 * (-SAC + 2 * SBC - SCC) \quad (6)$$

$$v_c = v_{dc}/3 * (-SAC - SBC + 2 * SCC) \quad (7)$$

e_a , e_b and e_c are three phase instantaneous AC voltages at the input of the current controlled converter and expressed as;

$$e_a = E_m \sin(\omega t), e_b = E_m \sin(\omega t - 2\pi/3) \text{ and } e_c = E_m \sin(\omega t + 2\pi/3) \quad (8)$$

Three phase reference currents (i_a^* , i_b^* and i_c^*) at the input to the current controlled converter are derived from the sensed three phase ac voltages (e_a , e_b , and e_c) and voltage regulator.

B. DC Link Voltage Regulator

The DC link voltage v^{\wedge} is sensed and is compared with the set reference voltage (V_{ref}). Voltage error (v_j , at nth sampling instant is expressed as;

$$v = V - v \quad M \quad n$$

The output of the PID [16] voltage regulator at the nth sampling instant is expressed as;

$$I_{1(n)} = I_{1(n-1)} + K_p * \{v_{ref(n)} - v_{ref(n-1)}\} + K_i * v_{el(n)} + K_d * \{v_{ref(n)} - 2.0 * v_{ref(n-1)} + v_{ref(n-2)}\} \quad (H)$$

Where, K_p , K_i , and K_d are proportional, integral and derivative constants, respectively, of the voltage regulator.

The output of the feedforward power estimator at nth sampling instant is $I_{2(n)}$. For the feedforward power control (Fig.1), DC link voltage $v.l$ and load current i , are sensed and processed in the output power estimator [10] to make available its output I_2 .

C. Current Template Formation

The unit current templates [8] are derived from sensed three phase AC voltages (e_a , e_b , and e_c) and a suitable phase shift ' ϕ ' given depending upon the desired level of power factor.

$$u_a = \sin(\omega t - \phi), u_b = \sin(\omega t - \phi - 2\pi/3) \text{ and } u_c = \sin(\omega t - \phi + 2\pi/3) \quad (12)$$

Where, ϕ is desired phase shift given to the unit current templates with respect to the corresponding voltages.

The angle ϕ may vary between $+90^\circ$ and -90° . However, in the present investigation ϕ is taken as zero for unity power factor operation of the converter.

D. Three Phase Reference Currents

The magnitude of the reference current is worked out at nth instant with the help of following relation.

$$I_m = I_{1(n)} + I_2(n) \quad (13)$$

The unit current templates (u_a , u_b and u_c) are multiplied with the I_m and thus the three phase reference currents are obtained;

$$i_a^* = I_m \sin(\omega t), i_b^* = I_m \sin(\omega t - 2\pi/3) \text{ and } i_c^* = I_m \sin(\omega t + 2\pi/3) \quad (14)$$

E. PWM Current Controller

These currents (i_a^* , i_b^* and i_c^*) are sinusoidal in nature and are free from harmonics. In order to have negligible injection of harmonics in the AC mains accompanied with the smooth operation of the converter, the currents (i_a , i_b and i_c) at the input to the converter must be closely tied with the reference currents (i_a^* , i_b^* and i_c^*). However, owing to the delay caused by R-L circuit at the input to the converter, three phase currents (i_a , i_b and i_c) through it are controlled within a closed vicinity of the reference currents (i_a^* , i_b^* and i_c^*). The concerned switching laws are derived in the following way:

- if $i_a < (i_a^* - hbi)$ switch S1 off and switch S4 on, SAC = 0
- if $i_a > (i_a^* + hbi)$ switch S1 on and switch S4 off, SAC = 1
- if $i_b < (i_b^* - hbi)$ switch S3 off and switch S6 on, SBC = 0
- if $i_b > (i_b^* + hbi)$ switch S3 on and switch S6 off, SBC = 1
- if $i_c < (i_c^* - hbi)$ switch S5 off and switch S2 on, SCC = 0
- if $i_c > (i_c^* + hbi)$ switch S5 on and switch S2 off, SCC = 1

According to this switching law, ON/OFF signals for the converters valves (S1, S2, S3, S4, S5 and S6) are generated. In response to this fast switching (ON/OFF), the currents (i_a , i_b and i_c) through the converter follow the reference currents (i_a^* , i_b^* and i_c^*). As seen from Fig.2, an IGBT in anti-parallel with the diode constitutes a valve.

F. Fuzzy PID Speed Controller

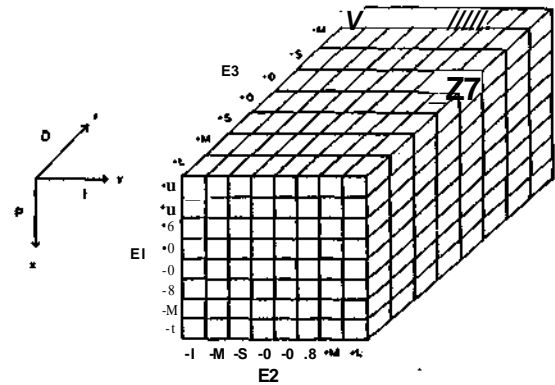
The Fuzzy PID speed controller has the internal structure of an expert system and it takes decision at each sampling instant. Its output is in terms of the reference torque T^* . The design of Fuzzy PID speed controller is briefly discussed here. The inputs to the Fuzzy PID speed controller are:

$$E1 = \omega_{ref} - \omega, E2 = \omega_{ref} \text{ and}$$

$$E3 = \omega_{ref} - 2 * \omega, M > \omega_{ref}$$

Depending upon error signals E1, E2 and E3 both in terms of trends (increasing or decreasing) and magnitudes, the Fuzzy controller searches the corresponding output from its linguistic codes table (TABLE I), which is of the order of 8X8X8. It could be appreciated that the many linguistic codes (117) entered into TABLE I of global fuzzy set have

TABLE I
GLOBAL FUZZY SET PRESENTATION



similar values for different conditions (values) of E1, E2 and E3. Therefore, the design of Fuzzy logic controller requires defuzzification and final linguistic codes are shown in TABLE II.

TABLE II
DEFUZZIFIED LINGUISTIC CODES IN TERMS OF NUMERICAL VALUES

Codes values	-L	-M	-S	-0	+0	+S	+M	+L
E1, E2, E3	-2.8	-2.0	-1.2	-0.6	0.6	1.2	2.0	2.8

The controller takes E1, E2 and E3 as its input and its output is the reference torque T^* .

G. Field Weakening Control

The estimated rotor speed (ω_r) is related to the magnetizing current vector (i_m^*) in the flux weakening block and necessary equations are given below;

$$i_m^* = \begin{cases} k \omega_r & \text{if rotor speed } < \text{ base speed of the motor} \\ k \omega_r \text{ At } & \text{if rotor speed } > \text{ base speed of the motor} \end{cases} \quad (15)$$

Where, i_m is the magnetizing current of the motor and k , is the flux weakening constant.

II. Field Orientation Control Structure

The system control structure computes the values of torque and flux producing components of the motor current. Therefrom, it computes three phase reference currents. The mathematical equations involved in this process are stated below;

$$i_{s^*} = r / (k i_{mr}) \tag{16}$$

$$i_{r^*} = r_r (di_{mr}/dt) + i_{in} \tag{17}$$

here, $k = (3 * \text{Poles} * M) / (2 * 2 * (1 + a))$

The slip speed could be expressed as

$$\omega_{s^*} = i_{r^*} / (\tau i_{mr}) \tag{18}$$

Here, M is the mutual inductance of the motor, r, is rotor circuit time constant and a, is the rotor leakage factor.

It is noted here that as long as the slip equation is being satisfied [S], the motor runs closely under the field oriented condition.

The currents i_{j^*} and i_{i^*} are in synchronously rotating reference frame, in order to convert them into stationary reference frame Park's transformation is applied. The quadrature currents in stationary reference frame are expressed as;

$$\begin{aligned} i_{u^*} &= i_{j^*} \cos \psi - i_{i^*} \sin \psi \\ i_{v^*} &= i_{j^*} \sin \psi + i_{i^*} \cos \psi \end{aligned} \tag{19}$$

The reference currents (i_{u^*} , i_{v^*} and i_{a^*}) are obtained with the help of following mathematical equations;

$$\begin{aligned} i_{u^*} &= i_{a^*} \\ v_{u^*} &= (\sqrt{3}/2) V - (1/2) i_{u^*} \\ v_{v^*} &= -(\sqrt{3}/2) V - (1/2) i_{v^*} \end{aligned} \tag{20}$$

Here, ψ is flux angle [4], it is computed as given here;

ψ at the nth sampling instant is given as

$$t_n = \psi |_{t_n} = \psi_0 + (\omega_r + \omega_s) X \tag{21}$$

Where, L, is the sampling period.

I. PWM Current Controller and Current Controlled Inverter

PWM current controlled voltage source inverter (Fig.3) is a variable frequency converter and it feeds power to the cage motor. The PWM pattern controlling the switching of the inverter devices, is generated by comparison of the motor currents (i_{u^*} , i_{v^*} and i_{a^*}) with their reference counterparts (i_{u^*} , i_{v^*} and i_{a^*}). As shown in Fig.3, the PWM current controller compares the motor current with the reference current and the resulting switching (ON/OFF) pattern governs the gates of the inverter devices (IGBT). The PWM switching frequency of the inverter devices is set at the value of 20 kHz. There are a total of eight combinations of the switches condition. The inverter devices ON/OFF conditions (switch function, SF) are stated as below:

- SF = 1 if upper device of inverter limb is on
- = 0 if lower device of inverter limb is on

Out of eight combinations of switches (power devices, IGBTs) each constitutes one space voltage vector. Therefore, as shown in Fig.4, there are in all eight space voltage vectors. Six space voltage vectors are of equal magnitude and they are 60° space displaced from each other and the remaining two are of zero magnitude. The switching functions (SFs) and the space phasor voltage vector are given in TABLE III.

TABLE III
SWITCHING FUNCTION AND SPACE VOLTAGE VECTORS

space Voltage vectors	Switch combination	Angle in degrees	SFA	SFB	SFC
V ₁	1	330-30	1	0	0
V ₂	2	30-90	1	1	0
V ₃	3	90-150	0	1	0
V ₄	4	150-210	0	1	1
V ₅	5	210-270	0	0	1
V ₆	6	270-330	1	0	1
V ₀	7	-----	0	0	0
V ₇	8	-----	1	1	1

The space voltage vectors (V[^]V_J) control the motor currents and are termed as the forcing functions or source voltages feeding power to the motor. In response to these space voltage vectors the currents

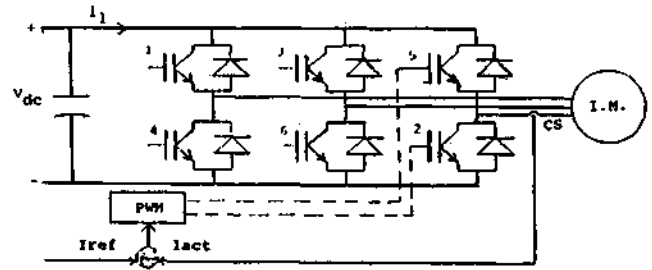


Fig.3 Schematic of PWM current controlled VSI through the motor windings are instantaneously controlled in a specified manner thereby, providing a fast dynamic response of the drive.

The power input to the motor is expressed as;

$$P_m = v_{u^*} i_{u^*} + v_{v^*} i_{v^*} + v_{a^*} i_{a^*} \tag{22}$$

Where, v_u, v_v and v_a are three phase voltage at the output of the inverter, these voltages have stepped waveform, however a filter makes them close to sinusoidal.

The load current on the converter (i_l) (eq.4) is expressed as;

$$i_l = P_m / v_{dc} \tag{23}$$

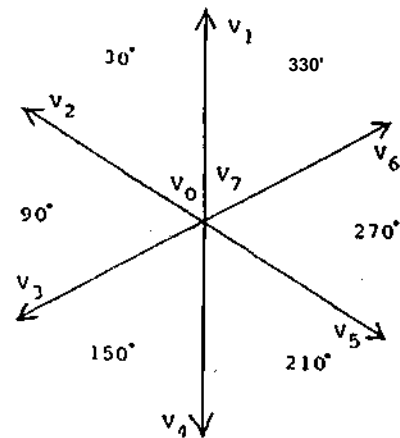


Fig.4 Space voltage vector representation

1. Induction Motor

The space voltage vectors resulting from the PWM switching

(ON/OFF) pattern maintain the desired pattern of the currents in the motor winding and the motor runs stably at the set speed. The volt-ampere equation of the induction motor results in a set of differential equations which is [18] given as:

$$p[i] = [L]^{-1}([v] - [R]i) - w_r[G](i) \quad (24)$$

The speed derivative from torque balance equation of the induction motor is expressed as;

$$pw_r = (T_r - T_e) * (\text{poles}/2) * (1/J) \quad (25)$$

Where $[v]$, $[i]$, $[R]$, $[L]$ and $[G]$ are voltage, current, resistance, transformer inductance and rotational inductance matrices. The p is the differential operator (d/dt), T_r is load torque, J is the moment of inertia of the shaft.

The electromagnetic torque T_e developed by the motor is expressed as:

$$T_e = (3/2) * (\text{poles}/2) * L_m * (v_{idc} - |v_r|) \quad (26)$$

Here L_m is a function of the magnetizing current and in order to take the magnetic saturation into account this particular function is given in the Appendix.

The set of the differential equations mentioned in equations (1), (2), (3), (4), (24) and (25) define the model of the system in terms of eight dependent variables such as i_d , i_q , v_{dc} , i_r^* , i_s , i_j , i_t and w_r and the time as the independent variable. A numerical technique namely Runge-Kutta method is found suitable for solving these differential equations. In order to study the response of the drive system and to have graphical representation of its behaviour, 'a' phase input current (i_a) and voltage (e_a), dc link voltage v_{dc} , the cage motor currents (i_s , i_w and i_j), electromagnetic torque T_e and speed w_r of the motor are stored.

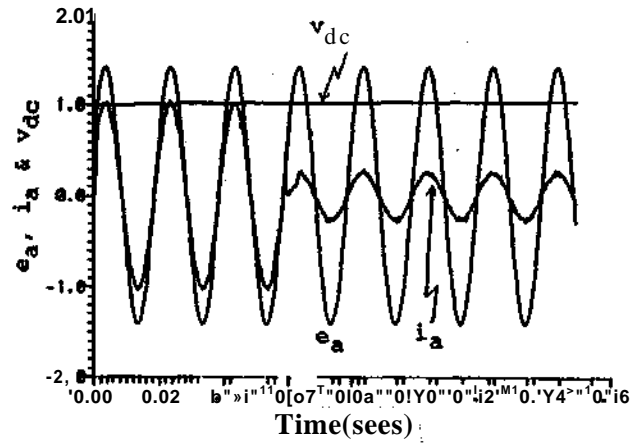
IV. RESULTS AND DISCUSSION

The model of the proposed drive system is simulated to investigate its dynamic performance and simulated results are shown in Figs.5-6. All the quantities shown in Figs.5 and 6 are given in per unit. However, their actual values are also given.

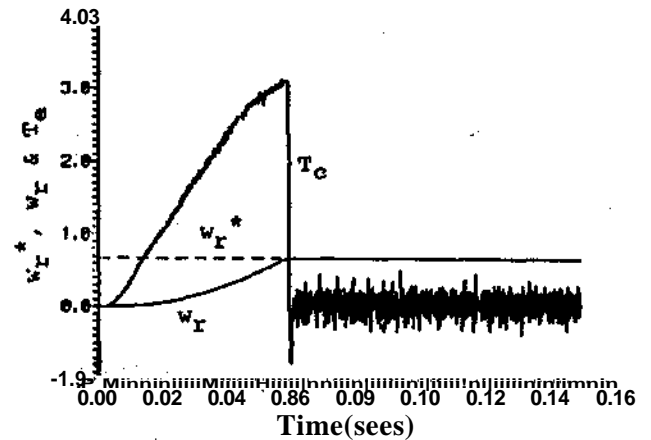
A. Starting Response of the Drive

Fig.5 shows the starting response of the drive: Initially the DC link is charged to its set value 1 p.u. (587 V). Starting command is given to the drive with a set speed of 0.67 p.u. (210 rads/sec). It is seen from Fig.5a that converter draws 1 p.u. (3.0 A) current at its input and the current is in phase with the voltage keeping the input power factor unity. The waveshape of the current at the input to the converter has perfect sinusoidal shape. While starting the drive the DC link voltage experiences a negligible (only $\pm 2\%$) fluctuations. Converter does not return any energy to the AC mains even if the voltage exceeds the set value. This is due to the demand of active energy by the induction motor during its starting. As soon as the motor is started, the excess trapped energy in the DC link causes reduction in the input currents. Moreover, if trapped energy exceeds a particular limit it causes a rise in the DC link voltage and the trapped energy is returned to the AC mains through regeneration. Finally after the DC link voltage reaches to its set value the amount of the current (0.2 p.u.) drawn at the input of the converter is just sufficient to cater to the needs of the induction motor. Current at the input to the converter during steady state is found sinusoidal.

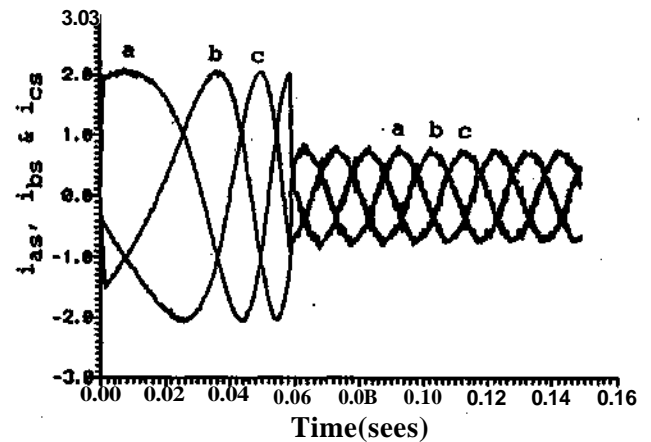
As it is seen from Figs.5b and c that the motor gets started in about 59 msecs. The fuzzy controller acts very accurately and keeps on updating the reference torque and the developed electromagnetic torque (T_e follows the T_r). Electromagnetic torque developed by the motor during its steady state no load running fluctuates to keep the motor speed tied with the set value. The motor draws only 2.2 p.u. (4.8 A peak) current during its starting, however, developed electromagnetic



(a)



(b)



(c)

Fig.5 Starting response of the drive system

torque is 3.1 p.u. (12.4 N-m). This happens as the motor is running in the vector control mode. No load running current is 0.7 p.u. (peak). The motor winding currents (Fig.5c) change quickly leading to its faster dynamic response.

B. Speed Reversal Response of the Drive

Fig.6 shows the speed reversal response of the drive. The motor is running in the forward direction at the set speed 0.67 p.u. (210 rads/sec). The current controlled converter is also drawing 0.1 p.u. at unity power factor. Momentarily the set speed is changed from +0.67 p.u. to -0.67 p.u., there is a regenerative braking (Fig.6a). The regeneration action reverses the direction of load current i , which makes

the current I , (Fig.1) also negative. Apart from this due to regeneration the DC link experiences a rise in voltage and the voltage controller makes the current I , also negative which helps I_2 . The currents I_1 and I_2 together make quickly the current I_m negative and as result the current at the input to the converter attains instantaneously 180° out of phase with respect to the voltage which leads a quick regeneration of the energy. The current controlled converter feeds this regenerative power to the AC mains.

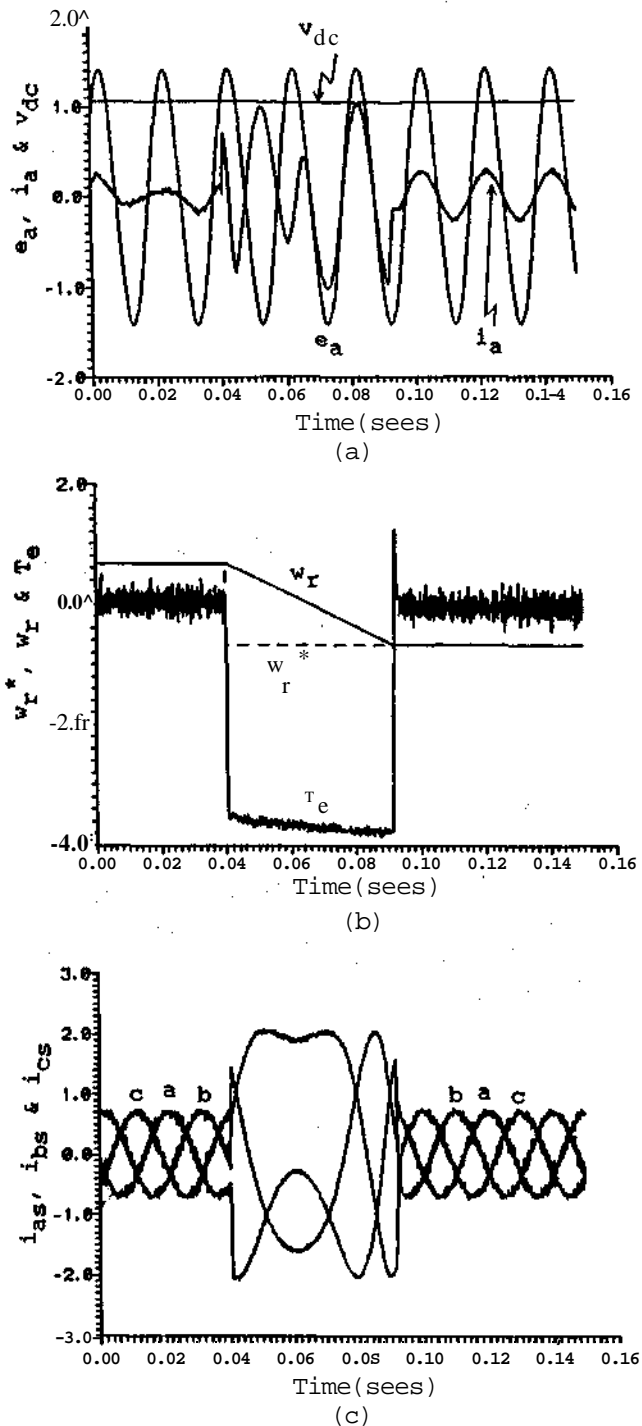


Fig.6 Speed reversal response of the drive system

As soon as the motor speed reaches zero and it starts speeding up in the reverse direction the active power demanded by it makes the current i , positive and hence I , also. Moreover, DC link may experience a dip in voltage which makes I , positive and once again I_1 and I_2 together make I_m , also positive. This makes input current to the converter in phase

with the voltage and the current controlled converter extracts the necessary power from the AC mains. The current at the converter input during braking and reverse motoring is found at the value of 1 p.u. (3.0 A peak). When the motor reaches a new set value of the speed converter current is settled down to the 0.2 p.u. which is sufficient to keep the DC link voltage to its set value as well as to meet out the induction motor no load losses.

It may be seen from Fig.6b that the time elapsed in the speed reversal operation of the drive is 52 msec only. The output of the fuzzy controller saturates to its rated value during speed reversal making the electromagnetic torque to jump 3.8 p.u., however, the currents drawn by the motor through the inverter during speed reversal operation are 2.2 p.u. (4.8 A peak). The fuzzy controller is activated as a result of the disturbance caused by the change in the set speed from a positive set value to the negative set value. The PWM current controller employed for the gating of the inverter devices quickly controls the motor currents giving the fast reversal of the drive. The current drawn by the motor are controlled ones owing to vector control the developed electromagnetic torque is sufficiently high and this brings the faster response in the drive.

V. CONCLUSIONS

The performance analysis of the proposed drive system has been carried out. It is found that during transients fuzzy controller instantaneously alters its output and this brings faster response in the drive. It is found that the feedforward power control of the converter has enhanced its response and has made the input current closer to sinusoidal aside from keeping the DC link voltage fluctuations in permissible limit ($\pm 2\%$). The current controlled converter-inverter link is found capable of providing four quadrant operation of the drive and it is found behaving as an ideal frequency changer. It is hoped that the proposed approach and system modeling presented in this investigation will be quite helpful to the researchers and practicing engineers. The proposed drive exhibits high performance and is suitable in a number of applications such as rolling mill, compressors, hoists applications, lifts, cranes, tractions, paper industry and textile industry.

VI. REFERENCES

- [1] Lipo T.A., "Recent progress in the development of solid-state ac motor drives", *IEEE Trans, on Power Electronics*, Vol.3, No.2, pp.105-117, Jan. 1988.
- [2] D.M.Brod and D.W.Novotny/Current control of VSI-PWM inverters", *IEEE Trans, on Industry Applications*, Vol. IA-21, No.3, pp.562-570, May/June 1985.
- [3] Xue Y., Xu X., Habetler T.G. and Divan D.M., "A low cost stator flux oriented voltage source variable speed drive", *Proceedings Industry Applications Society Meeting-1990*, pp.410-415, October 1990.
- [4] Bose B.K., *Power Electronics and AC Drives*, Prentice-Hall, Englewood Cliffs, New Jersey 07632, 1986.
- [5] Murphy J.M.D. and Turnbull F.G., *Power Electronics Control of A.C. Motors*, Pergamon Press, 1988.
- [6] Leonhard W., *Control of Electrical Drives*, Electric Energy System and Engineering Series, 1985.
- [7] Vas Peter, *Vector Control of AC Machines*, Clarendon Press Oxford, 1990.
- [8] Pan C.T. and Chen T.C., "Modelling and analysis of a three phase ac-dc converter without current sensor", *Proc. IEE Pt. B*, Vol.140, No.3, pp.201-208, May 1993.
- [9] B.T. Ooi, J.W. Dixon, A.B. Kulkarni and M. Nishimoto, "An integrated AC drive system using a controlled-current PWM rectifier/inverter link", *IEEE Trans, on Industrial Electronics*, Vol.3, No.1, pp.64-71, Jan. 1988.
- [10] Habetler T.G., "A space vector-based rectifier regulator for ac/dc/ac converters", *IEEE Trans, on Power Electronics*, Vol.8, No.1, pp.30-36, Jan. 1993.
- [11] Bose B.K., "Power electronics and motion control- technology

- status and recent trends", *IEEE Trans.on Industry Applications*, Vol.29, No.5, pp.902-909, Sept./Oct. 1993.
- [12] B.K. Bose, "Evaluation of modern power semiconductor devices and future trends of converters", *IEEE Trans, on Industry Applications*, Vol.IA-28, No.2, pp.403-413, March/April 1992.
- [13] Blaschke F., "The principle of field orientation as applied to the new transvector closed-loop control system for rotation field machine", *Siemens Review*, Vol. 34, p 217-220, 1972.
- [14] Amim Suyitno, J.Fujikawa, H.Kobayashi and Yasuhiko Dote, "Variable-structured robust controller by fuzzy logic of servomotors", *IEEE Trans, on Industrial Electronics*, Vol.40, No.1,pp.45-55, Feb.1993.
- [15] Cheng F.F. and Yell S.N., "Application of fuzzy logic in the speed control of ac servo system and an intelligent inverter", *IEEE Trans, on Energy Conversion*, Vol.8, No.2, pp.312-318, June 1993.
- [16] K.Minth Vu, "Optimal setting for discrete PID controllers", *Proc. IEE Pt.D*, Vol.139, No.1, pp.31- 40, Jan.1992.
- [17] Tang K.L. and Mulholland R.J., "Comparing fuzzy logic with classical controller designs", *IEEE Trans, on Systems, Man, and Cybernetics*, Vol.SMC-17, No.6, pp.1085-1087, Nov./Dec.87.
- [18] Krause P.C., *Analysis of Electric Machinery*, McGraw- Hill Book Company, 1987.

VII. APPENDIX

A. Converter Parameters

$R_c = 0.5$ Ohms, $L_K = 20$ inH, $C_d = 2000$ micro farad, 200V AC input, Maximum current input to the converter is 1.95 A (rms).

B. Motor Specifications

Cage rotor, 0.75kW, 3-Phase, 2-Pole, Y-Connected, 415V 50 Hz, $R_s = 9.45$, $R_r = 11.72$, $X_s = 11.04$, $X_r = 11.04$ (all in ohms/phase), $M = 0.678$ H, $J = 0.0018$ Kg-m²

The magnetizing inductance L_m is related to the magnetizing current (i_m) by the following manner:

For $i_m < 0.4$, $L_m = 1.32$

For $0.4 \leq i_m < 0.56$, $L_m = 1.32 - 1.5(i_m - 0.4)$

For $0.56 \leq i_m < 0.7$, $L_m = 1.07 - 1.07(i_m - 0.56)$

For $0.7 \leq i_m < 1.02$, $L_m = 0.92 - 0.56(i_m - 0.7)$

For $1.02 \leq i_m < 1.2$, $L_m = 0.74 - 0.33(i_m - 1.02)$

For $1.2 \leq i_m < 1.48$, $L_m = 0.68 - 0.40(i_m - 1.2)$

For $1.48 \leq i_m < 1.82$, $L_m = 0.57 - 0.2(i_m - 1.48)$

For $1.82 \leq i_m < 2.095$, $L_m = 0.5 - 0.15(i_m - 1.82)$

For $2.1 \leq i_m$, $L_m = 0.46$